

SEED-GROWING HEART SEGMENTATION IN HUMAN ANGIOGRAMS

Antonio Bravo, José Clemente

*Grupo de Bioingeniería, Decanato de Investigación, Universidad Nacional Experimental del Táchira
San Cristóbal 5001, Venezuela*

Rubén Medina

Grupo de Ingeniería Biomédica, Facultad de Ingeniería, Universidad de Los Andes, Mérida 5101, Venezuela

Keywords: Segmentation, Unsupervised clustering, Mean shift, Cardiac images, Human heart, Left ventricle.

Abstract: In this paper an image segmentation scheme that is based on combinations of a non-parametric technique and a seed based clustering algorithm is reported. The method has been applied to clinical unsubtracted angiograms of the human heart. The first step of the method consists in applying a mean shift-based filter in order to improve the left ventricle cavity information in angiographic images. Second, the initial seed is semi-automatically generated from the aortic valve manual localization by a specialist. Third, each angiographic image is segmented using a clustering algorithm that begins with the seed which is grown until image pixels associated to the left ventricle cavity are clustered. A validation is performed by comparing the estimated contours with respect to contours manually traced by a cardiologists. From this validation stage the maximum of the average contour error considering six angiographic sequences (a total of 178 images) is 7.30 %.

1 INTRODUCTION

Image segmentation methods are a prerequisite to efficiently analyze the cardiac function from image data acquired by X-Ray angiographic systems during cardiac exams. Information about the size and shape of heart cavities during the cardiac cycle could be extracted. The use of traditional segmenting procedures to cardiac images does not allow to obtain accurate results due to the complexity and variability of the anatomic shapes. Low contrast, noise, and non-uniformity of regional intensities are some of the problems associated with X-ray based cardiac imaging modalities.

Left ventricle (LV) cavity plays a major role in the heart dynamics since it pumps oxygenated blood to the entire body. Left ventricle angiograms are obtained from a medical imaging modality based on X-rays, after the injection of a contrast medium in the cavities of the heart aiming at enhancing the contrast with respect to other tissues. Such examination enables the assessment of morphology and function of the heart. Ventriculographic image analysis requires a precise description of ventricular shape in order to

quantify the parameters associated with the cardiovascular function (Kennedy et al., 1970) (Rabit, 2000) or alternatively for performing the visualization of this anatomical structure (Medina et al., 2004). LV volumes and ejection fraction (EF) are important indexes for clinical assessments of heart function (Yan et al., 1978). The accurate description of ventricular function is important, since cardiovascular disease (CVD) accounts for one third of the deaths in the world (WHO, 2002).

The general image segmentation problem involves the division of a dataset into groups of similar objects. Thus, image segmentation consists in determining the regions containing pixels that have similar properties (Jain et al., 1999). There are many different methods for cardiac image segmentation based on supervised learning methods (Suzuki et al., 2004; Oost et al., 2006) or unsupervised learning (learning without teacher) (Sui et al., 2001; Bravo and Medina, 2008). In general, these methods provided an accurate representation of ventricular borders, however, they are not yet fully validated and accepted by clinicians as a gold standard.

The goal of this research is the developing of

a left ventricle semi-automatic segmentation method based on unsupervised clustering. The performance of the proposed method is quantified by estimating the difference between the contours obtained by the our approach with respect to the contours traced by the cardiologist. The segmentation error is quantified by using a set of metrics that has been proposed and used in the literature (Suzuki et al., 2004; Bravo and Medina, 2008). The paper is organized as follows. First, the complete process that performs the segmentation of the LV is detailed. Then, experiments carried out to validate the method are presented, and the results obtained are discussed. Finally, future developments are proposed.

2 METHOD

2.1 Dataset

Six mono-plane angiograms acquired at several instants of the cardiac cycle are used to evaluate the proposed unsupervised clustering method for left ventricle cavity identification. The sequences of ventriculographic images are acquired with a Siemens X-Ray angiographic system, considering one standard examination view (right anterior oblique-RAO 30°), with a field of view (FOV) of 27 cm, a spacing between pixels of 0.285 mm, a frame rate of 25 images/s and a total acquisition time of 2 s. The spatial resolution of the image is 512 × 512, with a depth of 8 bits per pixel.

2.2 Image Enhancement

Non-parametric methods have been widely used in segmentation problems due to their robustness in statistical analysis. These methods estimate the data underlying distributions (unknown density function) without prior knowledge of the distributions structures (Fukunaga, 1990).

The mean shift procedure is a non-parametric technique that does not depend on any geometric model assumptions (Fukunaga and Hostetler, 1975). This procedure has been used in image processing tasks such as filtering and clustering (Comaniciu and Meer, 2002). The objective of the procedure is to estimate the density gradient based on kernel density estimation method (Parzen window technique). This density gradient is defined as the direction from a sample point towards the center of its cluster. The estimated density gradient ($\hat{\nabla}f(x)$) is used to obtain an estimation ($\hat{f}(x)$) of the unknown density function ($f(x)$). The main goal of the estimation is to characterize the

modes of the data distribution. These modes are computed by iteratively moving the data according to a mean shift vector calculated using (1).

$$\mathbf{m}_h(x) = \frac{1}{2}c h^2 \frac{\hat{\nabla}f_h(x)}{\hat{f}_h(x)} \quad (1)$$

where h is the bandwidth (smoothing kernel parameter) and c is the normalization constant.

According to (1) the mean shift vector in the point x is aligned with the local gradient of the estimated density function. The idea is to track the path leading x to the stationary point of the estimated density. The stationary points in the estimated density represent the modes of the data distribution. If the density function modes are considered cluster centers, the mean-shift filtering algorithm shrinks data points towards these centers. A filtering example is shown in Figure 1. An end-systole ventriculogram image (RAO view) is used to illustrate the preprocessing stage. This ventriculogram corresponds with the end-systole image of the patient after a surgical ventricular restoration (SVR) (Ferrazzi et al., 2006). In the filtered image (Figure 1.b) is shown that part of the patches of autologous or artificial material that are placed to close the defect are removed. Additionally, the left ventricle cavity information is enhanced.

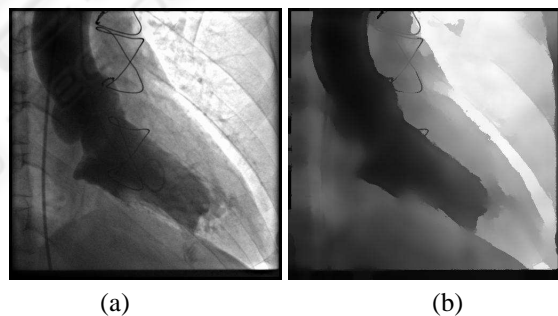


Figure 1: Enhancement process. (a) Original image. (b) Mean shift filtered image.

2.3 Segmentation Stage

A region growing technique is used to segment the LV. Region growing methods have been used for performing the segmentation of several medical imaging modalities (Lehmann et al., 2005). The region growing is usually based on simple linkage, on multiple connections or centroid based linkage (Haralick and Shapiro, 1992).

The unsupervised clustering algorithm proposed in this paper requires a seed point located inside the region of interest to identify the cardiac cavity. The seed is established in one angiographic projection (one time instant of the image sequence).

2.3.1 Seed Selection Procedure

The seed is used for starting the region-growing segmentation process. This seed is established in the 2-D image \mathbf{I}^t (t represents the time instant of the angiography dataset) according to following procedure:

1. A manual process performed by a cardiologist is applied to locate the aortic valve sides (VA and VP).
2. After the aortic valve points are identified, they are joined starting from the VA point and ending in the VP point using a straight line. The distance l between VA and VP points is computed.
3. The midpoint (V_M) of the line described by VA and VP points is computed. This midpoint is used to construct a new line perpendicular to the line described by VA and VP points.
4. The seed point is the one located at the distance l measured along the perpendicular line from the V_M point. This procedure must guarantee that y coordinate of the seed point is greater than y coordinate of the V_M point.

Figure 2 shows the seed selection procedure. A silhouette of the left ventricle contour is used to illustrate the selection procedure.

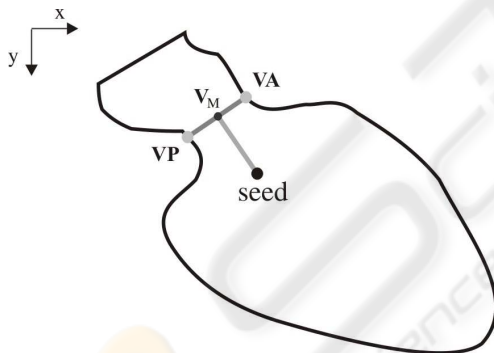


Figure 2: Seed point selection.

When the image \mathbf{I}^t has been segmented (process described in section 2.3.2) a binary image ${}^b\mathbf{I}^t$ is obtained. In this image, pixels in white represent the segmented region. From ${}^b\mathbf{I}^t$ the seed points necessary to segment the entire angiographic sequence are estimated. The center of mass of the segmented region in the image ${}^b\mathbf{I}^t$ is calculated and denoted as $r(x,y)$. The pixel $r(x,y)$ is the new seed to segment the image \mathbf{I}^{t+1} .

The procedure based on calculation of the center of mass, results in a point located very near of the LV anatomical axis. In consequence, the seed point is always located inside the target region (inside the LV).

2.3.2 Region Growing Algorithm

The algorithm is developed using dynamic linked-lists. The algorithm inputs are the enhanced image and a binary image with all pixels set to zero (0). The lists are implemented as a First In First Out (FIFO) queue. The list is used to store temporarily the pixels that fulfill the clustering criterion. The objective is to develop an iterative algorithm highly efficient with respect to memory requirements aiming at avoiding memory overflows. Each node in the list contains the pixel information: location and gray level intensity. The first node inserted in the list is the seed pixel. An overview of the proposed algorithm is shown on the flowchart in Figure 3. After introducing the seed in the FIFO list, the algorithm considers the following steps:

1. The first node of the list is dequeue.
2. The gray level information associated with the analyzed node is compared with pixel intensities in a 8 pixels neighborhood to determine if these neighbor pixels belong or not to the target region. The pixels of the neighborhood that fulfill the clustering criterion are inserted at the end of the list and their values in the binary image are modified to one (1). The pixels that do not fulfill the condition are rejected.
3. The algorithm continues with this process while there are nodes in the list. The algorithm output is the binary image where pixels values set to one represent the region of interest.

The uniformity criterion for grouping the pixels is as follows: pixels are grouped if the difference between the pixel value in the neighborhood and the intensity of the pixel extracted from the list is below $\frac{1}{8}$ of the standard deviation of pixels in the enhanced image.

2.3.3 Validation

In order to validate the proposed method, the difference between the estimated LV shape with respect to a ground truth shape, traced by an expert is quantified. A methodology to evaluate the LV segmentation method is considered. The approach proposed by Suzuki *et al.* (Suzuki et al., 2004) for evaluating the performance is incorporated. Suzuki's quantitative evaluation methodology is based on calculating two metrics that represent the contour error (E_C) and the area error (E_A). Equations (2) and (3) show the contour and area errors expressions.

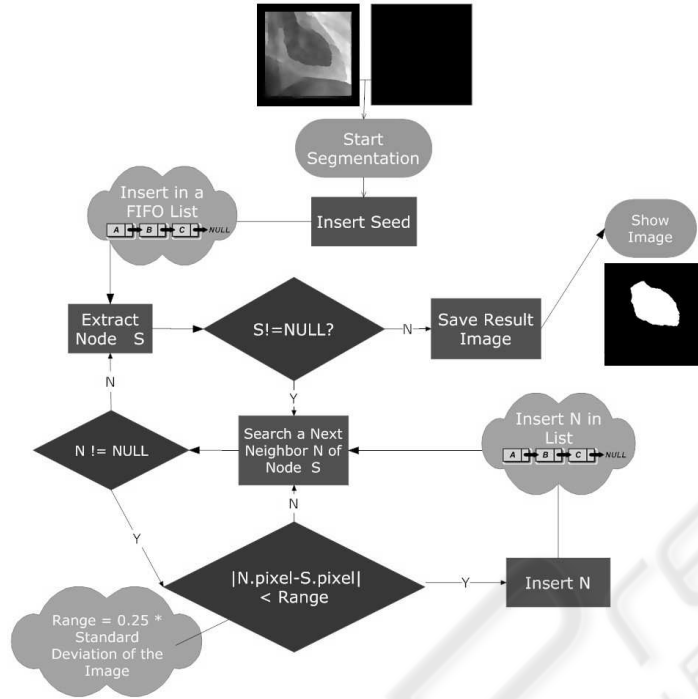


Figure 3: Clustering process.

$$E_C = \frac{\sum_{x,y \in R_E} [a_P(x,y) \oplus a_D(x,y)]}{\sum_{x,y \in R_E} a_D(x,y)}, \quad (2)$$

$$E_A = \frac{|\sum_{x,y \in R_E} a_D(x,y) - \sum_{x,y \in R_E} a_P(x,y)|}{\sum_{x,y \in R_E} a_D(x,y)}, \quad (3)$$

where:

$$a_D(x,y) = \begin{cases} 1, & (x,y) \in R_D \\ 0, & \text{otherwise} \end{cases}, \quad (4)$$

$$a_P(x,y) = \begin{cases} 1, & (x,y) \in R_P \\ 0, & \text{otherwise} \end{cases}, \quad (5)$$

where R_E is the region corresponding to the image support, R_D is the region enclosed by the contour traced by the cardiologist, R_P is the region enclosed by the contour obtained by our segmentation approach, and \oplus is the exclusive OR operator.

3 RESULTS

Figure 4 shows the results of the segmentation for six ventriculogram sequences. The contours traced by the cardiologist are represented by white dashdotted lines and the contours obtained with our approach are represented by black dashdotted lines. The first and third column show the end-systole images while the second and fourth column show the end-diastole images.

Tables 1–3 show a comparison of extracted contours with respect to the contours traced by the cardiologist. In these tables, the mean, the maximum (max), the minimum (min) and the standard deviation (std) for contour and area errors calculated according to Suzuki's metrics are shown.

Table 1 shows the errors for 178 images included in all ventriculographic sequences.

Table 1: Errors obtained for a total of 178 images processed.

	min	mean	max	std
E_A [%]	2.11	3.45	5.71	1.16
E_C [%]	4.24	7.30	10.38	2.45

Tables 2 and 3 show the errors obtained for end-diastole and end-systole images, respectively.

Table 2: Contour and area errors for end-diastole images.

	min	mean	max	std
E_A [%]	2.91	4.07	5.23	1.64
E_C [%]	4.99	6.86	8.72	2.63

The volume for the left ventricle during the cardiac cycle is estimated using the Area-Length method (Kennedy et al., 1970) from the contours obtained using the segmentation method. The correlation values between the clinical parameters (end-diastole volume

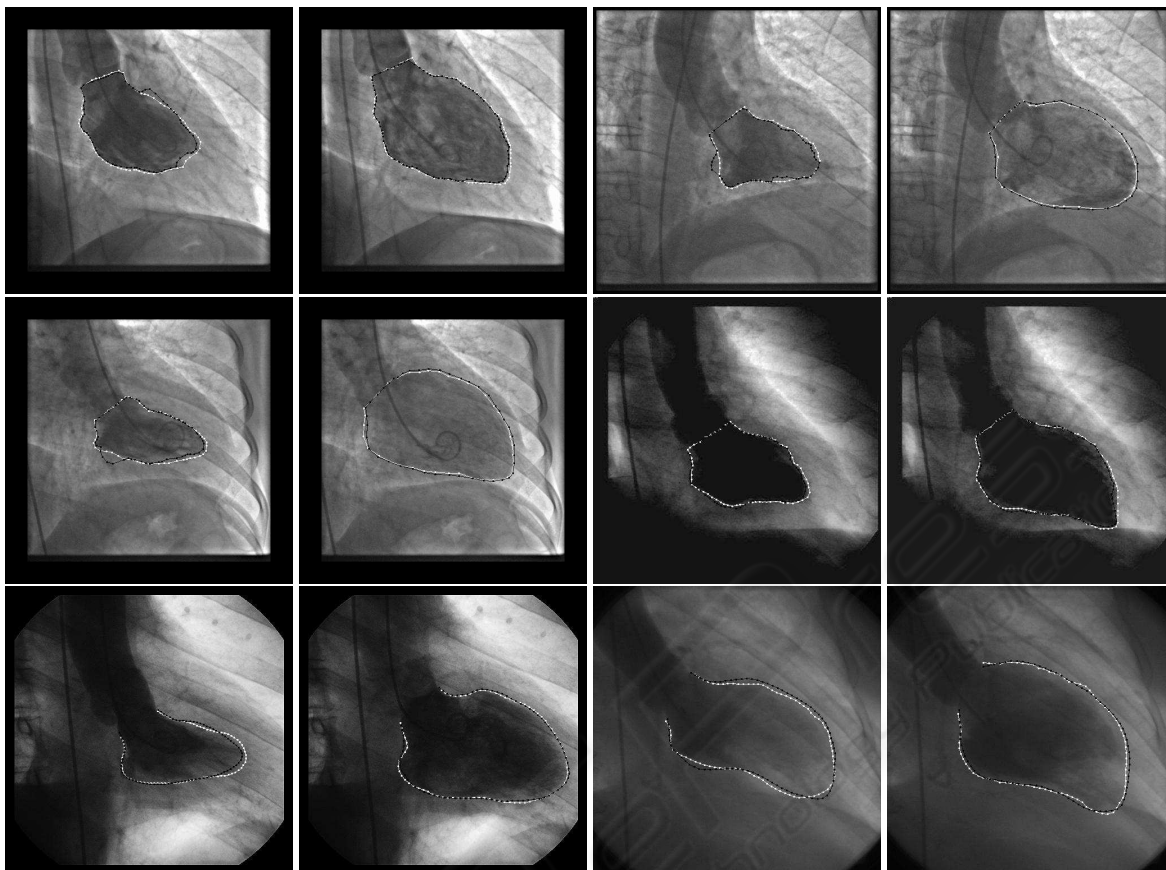


Figure 4: Results of LV segmentation. Ground truth (white dashdotted line) and estimated contour (black dashdotted line).

Table 3: Contour and area errors for end-systole images.

	min	mean	max	std
E_A [%]	2.19	3.37	4.16	1.07
E_C [%]	4.24	6.58	9.03	2.40

and end-systole volume) estimated using the LV contours obtained with the proposed method and those estimated from contours traced by a cardiologist was determined using the squared correlation coefficient. The correlation values were 0.9977 for end-diastole volume and 0.9983 for end-systole volume.

4 DISCUSSION

The approaches recently reported were based on quantifying only the errors at two cardiac instants: end-diastole and end-systole. In this research, we have estimated the segmentation error for all 152 images in the ventriculographic sequences. The average contour error obtained using our segmentation method was 7.30 % which is smaller than the av-

erage error for the end-diastole contour (6.2%) and end-systole contour (17.1%) reported by Suzuki *et al.* (Suzuki *et al.*, 2004). The average contour error for the end-diastole (4.1%) reported using the semi-automatic approach presented by Oost *et al.* (Oost *et al.*, 2006) is smaller than our value while the error at end-systole (12.8%) is greater. However, the average area error (3.45%) obtained by our method is smaller than the area errors reported in (Suzuki *et al.*, 2004; Oost *et al.*, 2006).

A strong correlation between the clinical parameters (end-diastole volume and end-systole volume) estimated using the left ventricle contours obtained with proposed method and those estimated with the contours traced by cardiologist was determined using the squared correlation coefficient.

Although our approach has been tested with a smaller number of sequences of images than the approaches recently reported, we have considered ventriculograms with complex pathologies.

5 CONCLUSIONS

A method for LV image segmentation from angiographic sequences was proposed. The pre-processing stage was based on a mean shift procedure aimed at performing the smoothing and enhancement of image contours. A region growing algorithm was controlled by a seed point located in an image at one time instant, which was propagated to the rest of instants in order to segment the entire angiographic sequence. The comparison was performed based on the methodology proposed in (Suzuki et al., 2004) which is also used in (Oost et al., 2006) and (Bravo and Medina, 2008). The validation stage shows that errors are small. The method allowed to detect LV important features such as the papillary muscles.

As a future work, a more complete validation is necessary, including a comparison of estimated parameters describing the cardiac function with respect to results obtained using MSCT image modality.

ACKNOWLEDGEMENTS

The authors would like to thank the Investigation Dean's Office of Universidad Nacional Experimental del Táchira and LOCTI grant PR0100401 for their support to this project.

REFERENCES

- Bravo, A. and Medina, R. (2008). An unsupervised clustering framework for automatic segmentation of left ventricle cavity in human heart angiograms. *Comput Med Imaging Graph.*, 32(5):396–408.
- Comaniciu, D. and Meer, P. (2002). Mean shift: A robust approach toward feature space analysis. *IEEE Trans. Pattern Anal. Machine Intell.*, 24(5):603–619.
- Ferrazzi, P., Matteucci, M., Merlo, M., Iacovoni, A., Rescigno, G., Bottai, M., Parrella, P., Lorini, L., Senni, M., and Gavazzi, A. (2006). Surgical ventricular reverse remodeling in severe ischemic dilated cardiomyopathy: the relevance of the left ventricular equator as a prognostic factor. *J Throac Cardiovasc Surg*, 131(2):357–363.
- Fukunaga, K. (1990). *Introduction to Statistical Pattern Recognition*. Academic Press Inc, USA.
- Fukunaga, K. and Hostetler, L. (1975). The estimation of the gradient of a density function, with applications in pattern recognition. *IEEE Trans. Inform. Theory*, 21(1):32–40.
- Haralick, R. and Shapiro, L. (1992). *Computer and Robot Vision*, volume I. Addison-Wesley Publishing Company, USA.
- Jain, A., Murty, M., and Flynn, P. (1999). Data clustering: a review. *ACM Comp. Surv.*, 31(3):264–323.
- Kennedy, J., Trenholme, S., Kaiser, I., and Wash, S. (1970). Left ventricular volume and mass from single-plane cineangiogram. A comparison of anteroposterior and right anterior oblique methods. *Am Heart J*, 80(3):343–352.
- Lehmann, T. M., Beier, D., Thies, C., and Seidl, T. (2005). Segmentation of medical images combining local, regional, global, and hierarchical distances into a bottom-up region merging scheme. In *Proceedings of SPIE*, volume 5747, pages 546–555.
- Medina, R., Garreau, M., Toro, J., Coatrieux, J. L., and Jugo, D. (2004). Three-dimensional reconstruction of left ventricle from two angiographic views: An evidence combination approach. *IEEE Transactions on Systems, Man, and Cybernetics—Part A: Systems and Humans*, 34(3):359–370.
- Oost, E., Koning, G., Sonka, M., Oemrawsingh, P. V., Reiber, J. H. C., and Lelieveldt, B. P. F. (2006). Automated contour detection in X-ray left ventricular angiograms using multiview active appearance models and dynamic programming. *IEEE Trans. Med. Imag.*, 25(9):1158–1171.
- Rabit, O. (2000). Quantitative analysis of cardiac function. In Bankman, I. N., editor, *Handbook of Medical Imaging: Processing and Analysis*, pages 359–374. Academic Press, San Diego.
- Sui, L., Haralick, R., and Sheehan, F. (2001). A knowledge-based boundary delineation system for contrast ventriculograms. *IEEE Trans. Inform. Technol. Biomed.*, 5(2):116–132.
- Suzuki, K., Horiba, I., Sugie, N., and Nanki, M. (2004). Extraction of left ventricular contours from left ventriculograms by means of a neural edge detector. *IEEE Trans. Med. Imag.*, 23(3):330–339.
- WHO (2002). Reducing risk and promoting healthy life. The World Health Report 2002 Geneva, World Health Organization.
- Yan, S., Lamberto, B., Vladir, M., and Harry, G. (1978). *From Cardiac Catheterization Data to hemodynamic Parameters*. F. A. Davis Company, USA.